New Results From H1

Olaf Behnke
on behalf of the
H1 Collaboration

Physikalisches Institut, Universität Heidelberg, Philosophenweg 12, 69120 Heidelberg, Germany

Abstract. A summary is given of some of the recent measurements made by the H1 Collaboration in ep collisions at HERA. These include studies of electroweak parameters, of proton charm and beauty structure functions, of α_s from the ratio of tri- to dijet cross sections, of diffractive scattering with dijets in the final state and of searches for strange pentaquarks. Also the first results from the analysis of HERA II e^+p and e^-p data are shown, including studies of events with isolated leptons and large missing transverse momentum and the first measurement of charged current cross sections with left handed polarised e^- beams.

PACS: 10.

INTRODUCTION

Recent measurements are summarised, which were made by the H1 Collaboration in the year leading up to the Deep Inelastic Scattering (DIS) Conference in Madison. First the results are presented which are obtained with the HERA I e^+p and e^-p data taken in the years 1994-2000, comprising an integrated luminosity of up to ~ 120 pb^{-1}. Second the results are shown which are made with the recent HERA II data with longitudinally polarised lepton beams, comprising up to ~ 74 pb^{-1} of integrated luminosity. Many further results, and more detail on the topics discussed here, can be found in the accompanying articles in these Proceedings. The H1 apparatus is described in detail in [1].

FIT OF ELECTROWEAK PARAMETERS

Electron proton scattering at HERA is dominated by photon exchange for the largest part of the covered phase space in momentum transfer Q^2. However one probes at HERA also the region where $\sqrt{Q^2}$ is approaching or exceeding the masses of the W and Z electroweak gauge bosons, and where the exchange of these bosons is of similar strength as the γ exchange. Necessary ingredients for calculating these processes are the quark densities in the proton and the electroweak parameters such as the coupling constants of the quarks to the gauge bosons. Using the e^+p and e^-p charged (W-exchange) and neutral current (γ and Z-exchange) cross sections previously measured by the H1 experiment [2, 3, 4, 5], a combined electroweak and QCD analysis is performed to determine electroweak parameters fully accounting for their correlations with proton parton distributions.

The *neutral current* measurements are used to determine for the first time at HERA the vector and axial coupling constants of the u and d quarks to the Z boson. The results are shown in figure 1. The sign ambiguities, which are present in the LEP e^+e^- results [6],

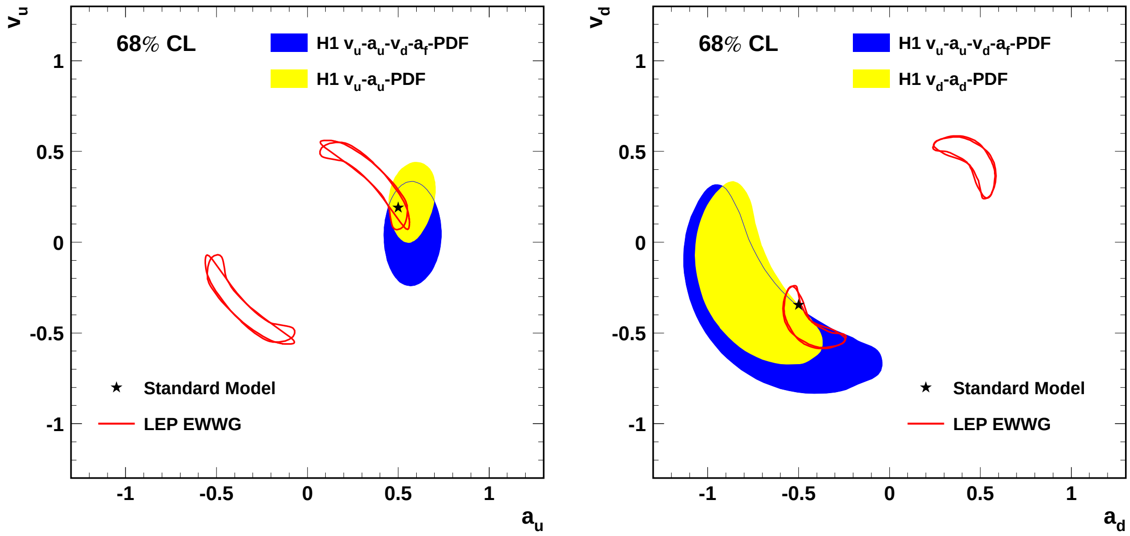

FIGURE 1. Results at 68% confidence level (CL) on the weak neutral current couplings of u (left plot) and d (right plot) quarks to the Z boson determined in the H1 measurement (the shaded contours) in comparison with those determined by the combined LEP data [6] which have both sign and $v-a$ exchange ambiguities. The dark-shaded contours correspond to results of a simultaneous fit of all four couplings whereas the lighted-shaded contours correspond to results of fits where either d or u quark couplings are fixed to their Standard Model (SM) values. The stars show the expected SM values.

as can be seen in figure 1, are unambiguously resolved. This is due to the fact, that at HERA the $\gamma - Z$ interference is probed over a wide range of Q^2. The obtained parameters are in good agreement with the expected Standard Model values.

The observed Q^2 shape of the *charged current* data is exploited to determine a W propagator mass with the result $M_{prop} = 82.87 \pm 1.82_{exp}\,^{+0.30}_{-0.16}|_{model}$ GeV. When analysing the data in the context of the Standard model, in the so-called-on-mass-shell (OMS) scheme [7], the Fermi constant G_F can be expressed in terms of M_Z and M_W and hence also the global normalisation of the data becomes sensitive to M_W. The corresponding fit result for M_W is translated into an indirect determination of sin^2_W, yielding $sin^2_W = 0.2151 \pm 0.0040_{exp}\,^{+0.0019}_{-0.0011}$.

The W exchange is also sensitive to the top mass through loop corrections. This is exploited to determine for the first time at HERA the top mass with the result $m_t = 108 \pm 44$ GeV, where the error covers only the experimental uncertainty.

PROTON STRUCTURE FUNCTIONS $F_2^{c\bar{c}}$ AND $F_2^{b\bar{b}}$

H1 presents at this conference measurements of inclusive charm and beauty cross sections in ep collisions at HERA over a wide range of momentum transfer $3.5 \leq Q^2 \leq 650\,\mathrm{GeV}^2$. The results at higher values of $Q^2 > 100$ GeV^2 have been recently published [8], the preliminary measurements at lower values of $Q^2 < 100\ \mathrm{GeV}^2$ are presented for the first time at this conference. The fraction of events containing charm and beauty quarks is determined using a method based on the impact parameter, in the transverse plane, of tracks to the primary vertex, as measured by the H1 vertex detector [9]. Values for the structure functions $F_2^{c\bar{c}}$ and $F_2^{b\bar{b}}$ are obtained. This is the first measurement of $F_2^{b\bar{b}}$. The results are shown in figure 2 as function of Q^2 in bins of the Bjorken scaling variable x. The measurements show positive scaling violations which

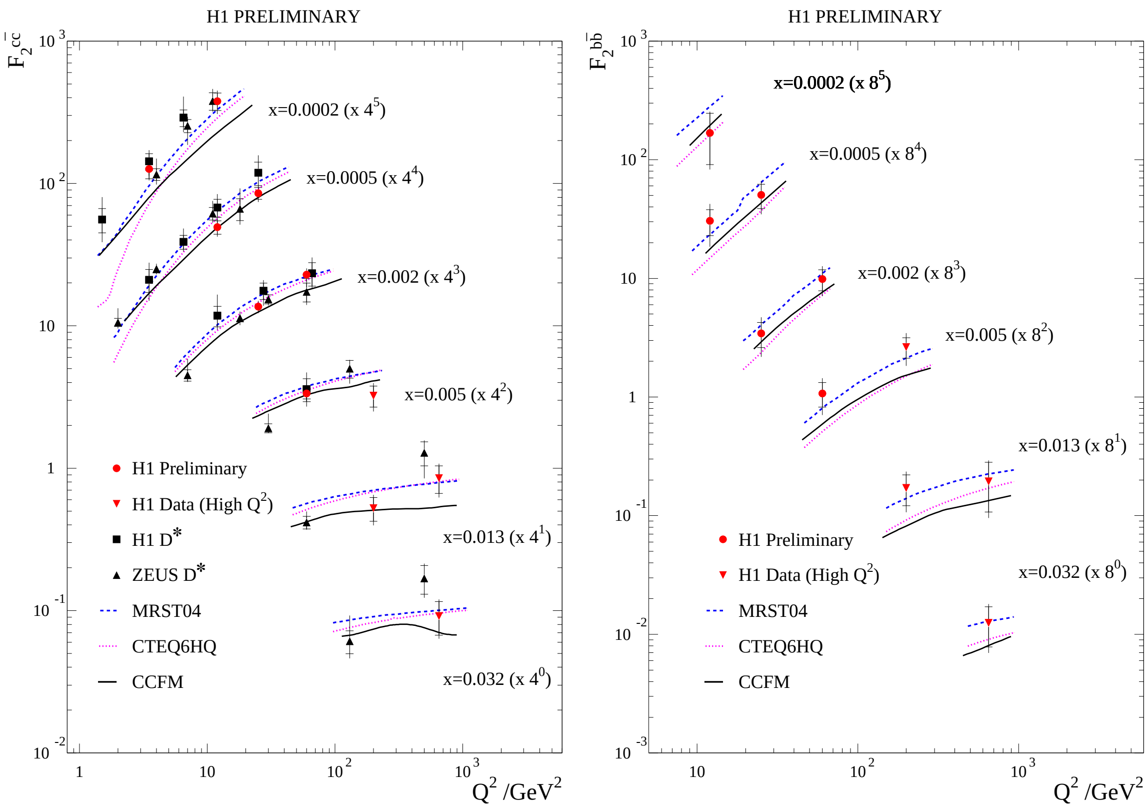

FIGURE 2. The measured $F_2^{c\bar{c}}$ (left) and $F_2^{b\bar{b}}$ (right) shown as a function of Q^2 for various x values. The inner errors bars show the statistical error, the outer error bars represent the statistical and systematic errors added in quadrature. The $F_2^{c\bar{c}}$ measurements obtained of D^* mesons from H1 [10] and ZEUS [11] and the predictions of different QCD model calculations are also shown.

increase with decreasing x. The charm measurements are in good agreement with the previous results extracted from D^* meson measurements by H1 [10] and ZEUS [11], which are also shown in figure 2 (left). The new measurements have the advantage of a high acceptance, which exceeds 70% in each Q^2 and x bin, both for charm and beauty. On the contrary, for the D^* measurements correction factors of typically > 2 have to be applied to extrapolate the data outside the D^* visible kinematic range, in order to obtain an inclusive charm cross section. The charm and beauty data are compared with several QCD model predictions. The next to leading order (NLO) perturbative QCD predictions by MRST [12] and CTEQ [13] use the variable flavour number scheme (VFNS). In this scheme at values of $Q^2 = M^2$ the dominant leading order process is $\gamma g \rightarrow q\bar{q}$, where

$q = c$ or b and where the gluon is emitted from the proton. As Q^2 increases, in the region $Q^2 \gg M^2$ the heavy flavour quarks are treated as massless partons in the proton and the leading order process is $\gamma q \to q$. The calculations by MRST and CTEQ differ in the way the transition between the two regimes is dealt with. This leads to significant differences between the two predictions in the kinematic range of this measurement, especially for beauty as can be seen in figure 2. However, within the experimental uncertainties both calculations describe the new data well, both for charm and beauty.

In the kinematic region of this measurement, the charm contribution to the total ep cross section, i.e. the ratio $F_2^{c\bar{c}}/F_2$ is found to be around 20%-30% and increases slightly with increasing Q^2 and decreasing x. The beauty contribution to the total ep cross section increases rapidly from $\leq 0.4\%$ at $Q^2 = 12$ GeV^2 to $\sim 5\%$ at $Q^2 = 650$ GeV^2.

QCD TESTS WITH FINAL STATES

Determination of α_s from three to two jet ratio

H1 presents at this conference a new determination of the strong coupling constant α_s via the ratio $R_{3/2}$ of tri- to dijet cross sections in deep inelastic scattering. The measurement is performed over a range of momentum transfer $150 < Q^2 < 150000$ GeV^2 and transverse jet energies $5 < E_T < 50$ GeV. Jets are defined by the inclusive $k_\perp$ algorithm in the Breit frame. Figure 3 shows the measured dijet and trijet differential cross sections as function of Q^2. The data are compared to an NLO prediction using the NLOJET++

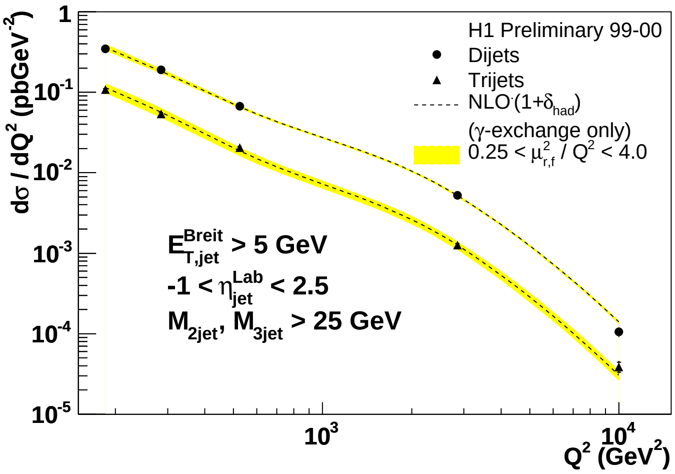

FIGURE 3. Neutral current di- and trijet differential cross sections, with respect to Q^2, shown with NLO pQCD predictions including hadronisation corrections. The shaded bands show the effect of varying the renormalisation/factorisation scale by a factor of two. The highest Q^2 bin is overestimated by the theoretical predictions due to the absence of electroweak effects in the NLO calculations.

program [14], which describes the data very well with the exception of the highest Q^2 bin. The cross section in this bin is overestimated by the theoretical predictions due to

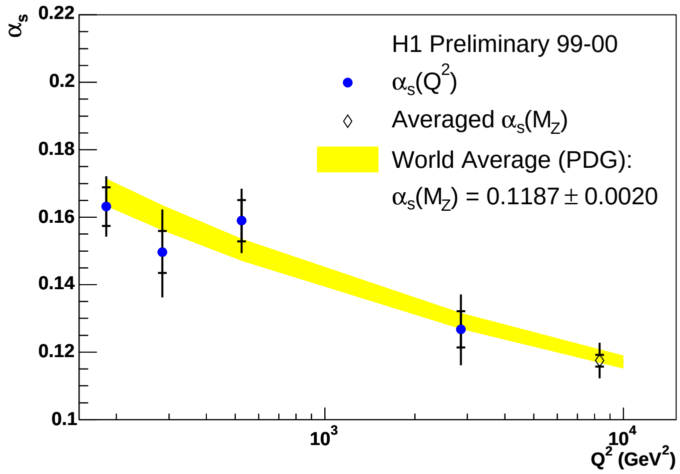

FIGURE 4. $\alpha_s(M_Z)$ values, from each Q^2 bin, as determined from a fit to the ratio of tri- to dijet cross section in that bin, evolved to their values at their respective values of Q^2 (triangles) using the two-loop solution of the renormalisation group equation. Uncertainties shown are statistical up to the horizontal bar, and then the quadratic sum of statistical and systematical uncertainties. The averaged value of $\alpha_s(M_Z)$, found using a χ^2 minimisation fit, is shown at the far right (empty diamond). The evolution of the current world average value of $\alpha_s(M_Z)$ is shown as a shaded band.

the absence of electroweak effects in the NLO calculation. For this reason the highest Q^2 bin is omitted in the current determination of α_s, which is discussed in the following.

For each bin in Q^2 a value of $\alpha_s(M_Z)$ is determined by matching the theoretical prediction from NLOJET++ as function of $\alpha_s(M_Z)$ to the measured ratio $R_{3/2}$ in that bin. Figure 4 shows the $\alpha_S(M_Z)$ values from each Q^2 bin evolved to their values at their respective values of Q^2. The data are in agreement with the predicted evolution by pQCD. An overall value of $\alpha_s(M_Z)$ is calculated from the weighted average of the $\alpha_s(M_Z)$ measurements in the bins and is also shown in figure 4 (right-most point). The result is $\alpha_{s(M_Z)} = 0.1175 \pm 0.00017$ (stat.) ± 0.0050 (syst.) $^{+0.0054}_{-0.0068}$ (th.), which is in good agreement with the world average value $\alpha_s(M_Z) = 0.1187 \pm 0.0020$. The value is competitive with results from other experimental procedures from different processes and is in agreement with the result recently obtained from $R_{3/2}$ by the ZEUS collaboration [15].

Diffraction

QCD predicts that the cross section for diffractive DIS factorises into universal diffractive parton densities (DPFDs) and process-dependent hard scattering coefficients [16] Diffractive parton densities have been determined from QCD fits to inclusive diffractive HERA data [17, 18]. Final state configurations for which a partonic cross section is perturbatively calculable in QCD include dijet production, which is directly sensitive to the gluon component of the diffractive exchange. However, applying this approach to predict diffractive dijet production in $p\bar{p}$ collisions at the Tevatron leads to an overestimation of the observed rate by nearly one order of magnitude [19]. This discrepancy has been attributed to the presence of the additional beam hadron remnant in $p\bar{p}$ collisions, which leads to secondary interactions and a breakdown of factorisation. The transition from DIS to hadron-hadron scattering can be studied at HERA in a comparison of scattering processes in DIS and in photoproduction. While in DIS the virtual photon always directly enters the hard interaction, in photoproduction the real photon can directly interact or be first resolved into partons which then initiate the hard scattering, resembling hadron-hadron scattering. H1 presents at this conference measurements of differential dijet cross sections both in diffractive DIS ($Q^2 > 4$ GeV^2 and in photoproduction ($Q^2 < 0.01$ GeV^2). The DIS results are in good agreement with QCD factorisation. In photoproduction, however, the dijet rate is suppressed by about a factor 0.5 compared to the NLO QCD prediction. This can be seen in figure 5, which shows the differential cross section in photoproduction as function of the quantities $z_{I\!P}^{\mathrm{jets}}$ and x_γ^{jets}.

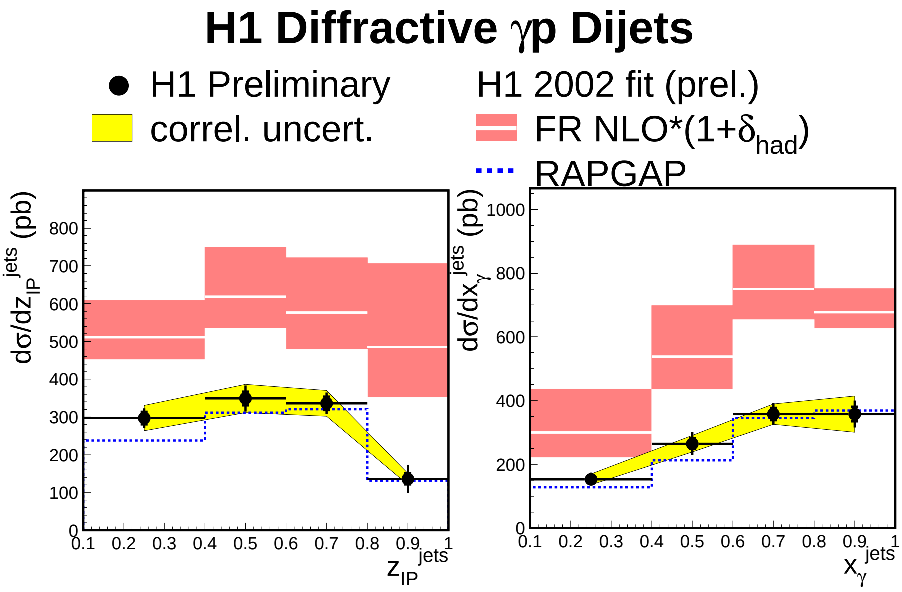

(a) (b)

FIGURE 5. Cross section for the diffractive production of two jets in photoproduction as a function of a) $z_{I\!P}^{\mathrm{jets}}$ and b) x_γ^{jets}.The band around the NLO prediction with hadronisation correction indicates the uncertainty resulting from the variation of the renormalisation scale by factors 0.5 and 2.

In the leading order picture $z_{I\!P}^{\mathrm{jets}}$ and x_γ^{jets} are the momentum fractions of the diffractive exchange and the photon, respectively, which are transferred into the dijet system. Surprisingly not only the region of $x_\gamma^{jets} < 0.9$, where resolved photon processes are expected to be enhanced but also the complementary region $x_\gamma^{jets} > 0.9$, where the direct photon contributions are expected to dominate, are suppressed at a similar level. Thus these preliminary results are suggestive of a breakdown of factorisation in photoproduction for both direct and resolved photon interactions.

SEARCH FOR STRANGE PENTAQUARK RESONANCE

Recently several experiments have published evidence for the production of a strange pentaquark θ^+ by various reaction processes [20, 21, 22]. It has been observed via its decays into K^+n and into $K_s^0 p$. Negative preliminary results, however, have been reported [23] from pp collisions, e^+e^- annihilation and also from fixed target photo-production experiments. H1 presents at this conference preliminary results on the search for the θ^+ decaying into $K_s^0 p$ in DIS, where the ZEUS experiment has found evidence of a signal at a mass of 1.522 GeV [22].

The identification of the decay protons is based on the measured energy loss in the central jet chambers. The invariant $K_s^0 p$ mass distribution obtained by the H1 experiment is shown in figure 6 for three different regions of Q^2 between 5 and 100 GeV^2.

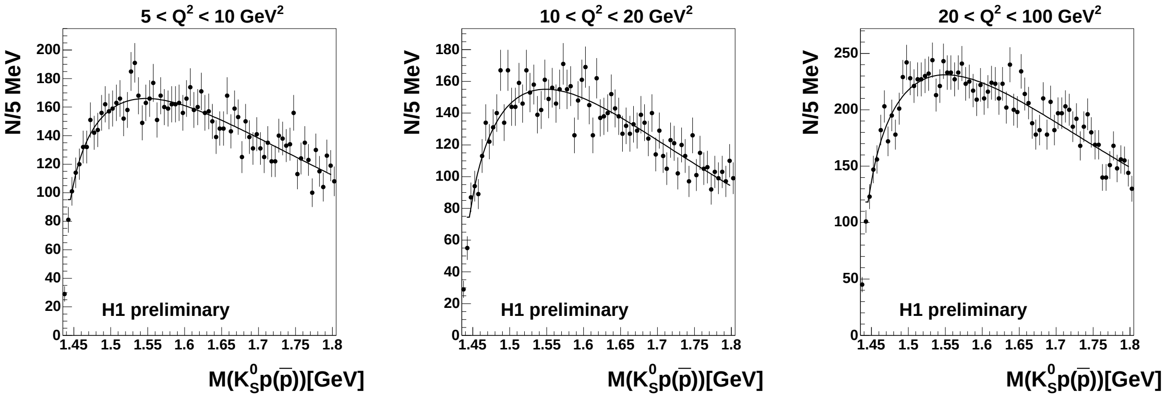

FIGURE 6. Invariant $K_S^0 p(\bar{p})$ mass spectra for the standard dE/dx selection, in three bins of Q^2. The full line shows the result from the fit of a background function to the data. The mass spectra show upward and downward fluctuations but no significant peak is observed.

The mass spectra do not show any significant signal in the mass range from threshold up to 1.7 GeV/c^2. With the assumption that pentaquarks are produced by fragmentation, mass dependent upper limits on the visible $\theta^\pm$ production cross sections are obtained for the investigated different kinematic regions. When repeating the analysis with similar cuts as were applied for the ZEUS measurement, no signal is observed either, although the sensitivity is expected to be comparable for both experiments.

RESULTS WITH HERA II DATA

Isolated lepton events with large missing transverse momentum

One of the most exciting results from HERA I is an excess observed in the H1 data [24] for events with an isolated lepton and large missing transverse momentum as this might be a hint for new physics beyond the standard model. The main contribution from the standard model to these events is the production of a real W boson (radiated from a quark) and the subsequent decay into lepton neutrino. An excess over the predicted cross sections was observed both for the electron and muon channel for large hadronic transverse momenta $p_T^X > 25$ GeV. For this conference H1 has updated the measurement with the available HERA II data. Six new electron events are found in these data but no new muon event. The yield of isolated electrons is again in excess over the standard model prediction. One of the new electron events is shown in figure 7.

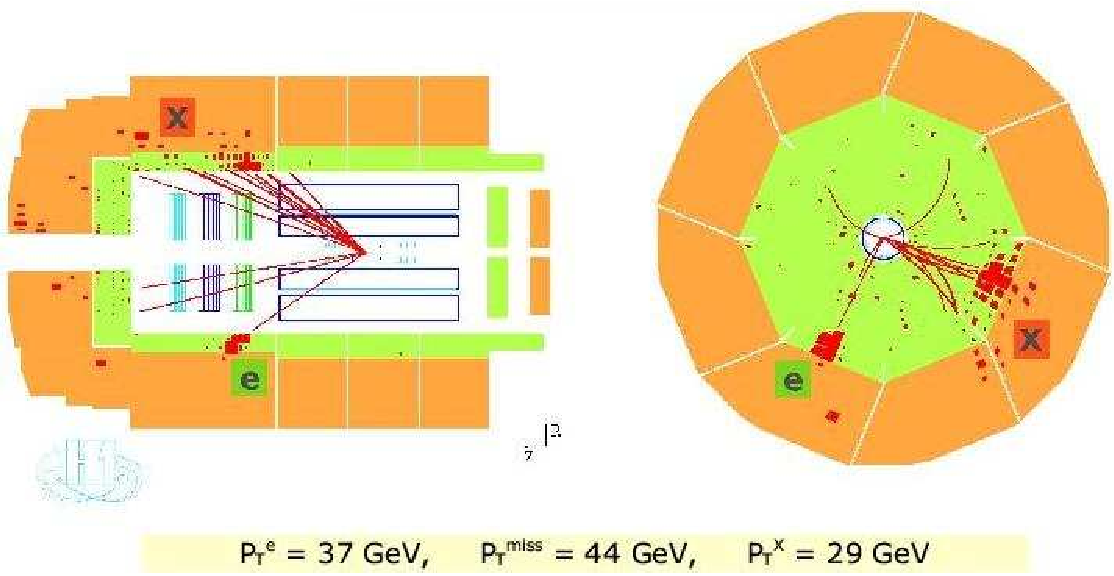

FIGURE 7. Display of an event with an isolated electron, missing transverse momentum and a prominent hadronic jet.

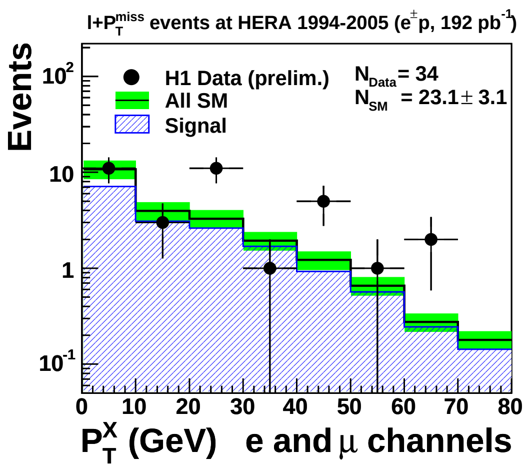

FIGURE 8. The hadronic transverse momentum distribution in the electron and muon channels combined: data (full HERA data set, $\mathscr{L} = 192$ pb^{-1}) is compared to the Standard Model expectation (open histogram). The signal component of the SM expectation, dominated by real W production, is given by the hatched histogram. N_{Data} is the total number of data events observed, N_{SM} is the total SM expectation. The total error on the SM expectation is given by the shaded band.

Figure 8 shows the observed event yield, when combining the electron and muon channel and exploiting the full HERA data set of e^+p and e^-p collisions from 1994-2005, as function of p_T^X. The numbers which are given in the figure legend correspond to the total p_T^X range. In the restricted region $p_T^X > 25$ GeV, there are 17 events observed while the SM predicts only 5.8.

Charged current cross sections with polarised e^- and e^+ beams

Since November 2004 the H1 and ZEUS experiments started to take for the first time data with with longitudinally polarised electron beams. This allows for a more detailed test of the electroweak part of the Standard Model at the energy frontier. The Standard model predicts that the cross sections for the charged current (CC) interactions $ep \to \nu X$ should have a linear dependence on polarisation, and furthermore, the cross section for fully right handed electrons should be zero (similarly for fully lefthanded positrons). This follows from the abesence of right handed currents within the framework of the Standard Model. At this conference H1 presents the first measurement of the total CC cross section for longitudinally polarised lefthanded electrons. The data set presented here has a mean lefthanded polarisation of (-25.40 ± 0.44)% and comprise an integrated luminosity of ~ 18 pb^{-1}. The measurement requires an excellent control of the energies deposited in the calorimeter, which is obtained by an *in-situ* calibration using a high statistics Neutral Current sample. Figure 9 shows the measured dependence of the e^+p and e^-p CC cross section with the lepton beam polarisation. The new measurement with the lefthanded electron beam enters as the circle point. The figure also shows two data points (triangles) with polarised positron beams and the results for unpolarised beams from the HERA I data [4, 5]. The data point with an average polarisation of -40% is the new and first CC measurement with a lefthanded polarised positron beam. This measurement is based on data from 2004 and was made preliminary [25] in summer 2004. All the data points are in good agreement with the standard model expectation.

CONCLUSION

The H1 Collaboration is completing the analysis of the HERA I data. At this conference many new and even some completely novel measurements with these data are presented such as the first determination at HERA of the axial and vector couplings of u and d quarks to the Z-boson and the measurement of the charm and beauty contribution to the total inclusive ep scattering using a secondary vertex tagging method. First results are obtained with the recent HERA II data. The HERA operation in the last few months leading up to this conference, with left handed polarised electrons, is exploited to make the first measurement of charged current events $ep \to \nu X$ for such polarised electrons. The excess observed in the HERA I data of events with an isolated lepton and missing transverse momentum is continued to be seen in the HERA II data. Six new candidates have been observed in the electron channel but none in the muon channel. To draw further conclusions, a much higher integrated luminosity is needed. This is expected to be provided in the next years of HERA II running and will allow a wealth of new and interesting measurements to be made at HERA.

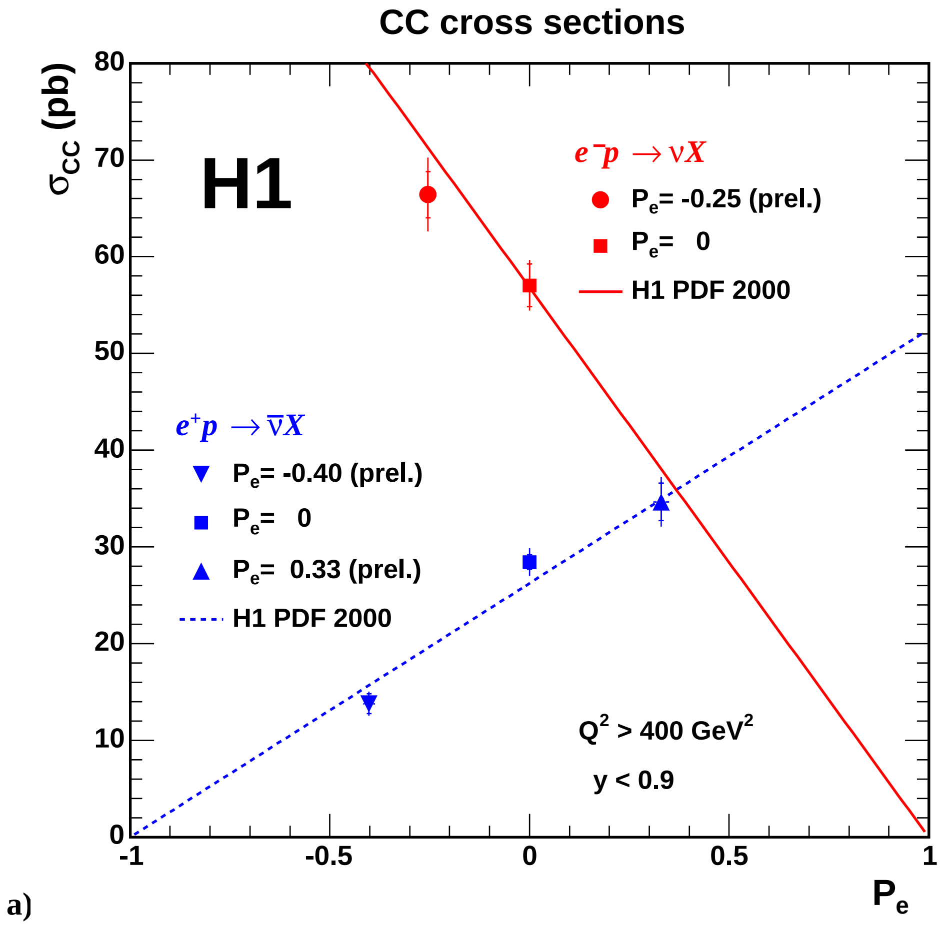

FIGURE 9. The dependence of the e^+p and e^-p CC cross section with the lepton beam polarisation P_e is shown. The data are compared to the prediction from the H1 PDF 2000 fit for polarised positrons (dashed line) and for polarised electrons (full line).

Many more results and details than presented in this summary talk can be found in these proceedings from the parallel sessions contributions.

ACKNOWLEDGEMENTS

I thank all of my H1 colleagues for their hard work which has resulted in the production of the measurements discussed here. Thanks to the H1 colleagues who helped me with the preparation of this talk, especially to Max Klein. I thank the DIS05 organisers for a pleasant workshop.

REFERENCES

1. I. Abt *et al.* [H1 Collaboration], Nucl. Instrum. Meth. A **386** (1997) 310.
2. C. Adloff *et al.* [H1 Collaboration], Eur. Phys. J. C **21**, 33 (2001) [arXiv:hep-ex/0012053].
3. C. Adloff *et al.* [H1 Collaboration], Eur. Phys. J. C **13**, 609 (2000) [arXiv:hep-ex/9908059].
4. C. Adloff *et al.* [H1 Collaboration], Eur. Phys. J. C **30**, 1 (2003) [arXiv:hep-ex/0304003].
5. C. Adloff *et al.* [H1 Collaboration], Eur. Phys. J. C **19**, 269 (2001) [arXiv:hep-ex/0012052].
6. LEP EW working group, http://lepewwg.web.cern.ch/LEPEWWG/plots/summer2004/.
7. A. Sirlin, Phys. Rev. D **22**, 971 (1980) and ibid. D **29**, 89 (1984).
8. A. Aktas *et al.* [H1 Collaboration], Eur. Phys. J. C **40**, 349 (2005) [arXiv:hep-ex/0411046].
9. D. Pitzl *et al.*, Nucl. Instrum. Meth. A **454**, 334 (2000) [arXiv:hep-ex/0002044].
10. C. Adloff *et al.* [H1 Collaboration], Phys. Lett. B **528**, 199 (2002) [arXiv:hep-ex/0108039].
11. S. Chekanov *et al.* [ZEUS Collaboration], Phys. Rev. D **69**, 012004 (2004) [arXiv:hep-ex/0308068].
12. A. D. Martin, R. G. Roberts, W. J. Stirling and R. S. Thorne, Eur. Phys. J. C **39**, 155 (2005) [arXiv:hep-ph/0411040].
13. S. Kretzer, H. L. Lai, F. I. Olness and W. K. Tung, Phys. Rev. D **69**, 114005 (2004) [arXiv:hep-ph/0307022].
14. Z. Nagy and Z. Trocsanyi, Phys. Rev. Lett. **87**, 082001 (2001) [arXiv:hep-ph/0104315].
15. S. Chekanov *et al.* [ZEUS Collaboration], arXiv:hep-ex/0502007.
16. J. C. Collins, Phys. Rev. D **57**, 3051 (1998) [Erratum-ibid. D **61**, 019902 (2000)] [arXiv:hep-ph/9709499].
17. C. Adloff *et al.* [H1 Collaboration], Z. Phys. C **76**, 613 (1997) [arXiv:hep-ex/9708016].
18. H1 Collaboration, paper 980 submitted to Intl.Conf. on High Energy Physics, ICHEP2002, Amsterdam.
19. T. Affolder *et al.* [CDF Collaboration], Phys. Rev. Lett. **84**, 5043 (2000).
20. T. Nakano *et al.*, (LEPS), Phys. Rev. Lett. **91** (2003) 012002;
    S. Stepanyan *et al.*, (CLAS), Phys. Atom. Nuclei **66**, 1715 (2003);
    J. Barth *et al.*, (SAPHIR), Phys. Lett. B **572** (2003) 127;
    V. Kubarovsky *et al.*, (CLAS), Phys. Rev. Lett. **92** (2004) 03201 [erratum-ibid. 92 (2004) 049902].
21. V. V. Barnim *et al.*, (DIANA), Phys. Atom. Nucl. **66** (2003) 1715 [Yad. Fiz. 66 (2003) 1763];
    A. E. Asratyan, A. G. Dolgolenko and M. A. Kubantsev, Phys. Atom. Nucl. **67** (2004) 682;
    A. Aleev *et al.*, (SVD), hep-ex/0401024;
    A. Airapetian *et al.*, (HERMES), Phys. Lett. B **585** (2004) 213;
    M. Abdel-Bary *et al.*, (COSY-TOF),Phys. Lett. B **595** (2004) 127.
22. S. Chekanov *et al.* [ZEUS Collaboration], Phys. Lett. **591** (2004) 7.
23. J. Z. Bai *et al.*, (BES), Phys. Rev. D **70** (2004) 012004;
    BaBar Collaboration, hep-ex/0408064;
    BELLE Collaboration, hep-ex/0409010;
    S. R. Armstrong, hep-ex/0410080; S. Schael *et al.*, (ALPEH), Phys. Lett. B **599**(2004) 1;
    I. Abt *et al.*, (HERA-B), Phys. Rev. Lett. **93** (2003) 212003;
    Yu. M. Antipov *et al.*, (SPHINX), Eur. Phys. J. A **21**, 455 (2004);
    M. J. Longo *et al.*, (HyperCP), Phys. Rev. D **70** (2004) 111101;
    D. O. Litvintsev, (CDF), hep-ex/0410024;
    R. Mizuk *et al.*, (Belle), hep-ex/0411005;
    C. Pinkerton *et al.*, (PHENIX), J. Phys. G **30** (2004) 1201;
    R. De Vita, (CLAS Collaboration), *Search for pentaquarks at CLAS in photoproduction from protons*,American Physical Society Meeting, Tampa, Florida, April 2005.
24. V. Andreev *et al.* [H1 Collaboration], Phys. Lett. B **561**, 241 (2003) [arXiv:hep-ex/0301030].
25. H1 Collaboration , Contributed paper no. 756/758 to ICHEP04,
    http://www-h1.desy.de/h1/www/publications/htmlsplit/H1prelim-04-141.long.html.